22nd International Conference
ENGINEERING MECHANICS 2016
Svratka, Czech Republic, 9 – 12 May 2016

WING TIP VORTEX RANS AND LES SIMULATION AND MEASUREMENT OF THE MEAN CHARACTERISTICS

J. Matějů[*], P. Griffin[**], J. O'Brien[***], P. Zikmund[****]

Abstract: *LES, RANS SST $k-\omega$ and uRANS − RST simulation of mean wing tip vortex characteristics at x/c = 6 position were compared to experiments. The wing tip vortex was generated by a wing at $AoA = 10\,deg$, $U_\infty = 34\,m \cdot s^{-1}$, $Re = 3.22 \times 10^5$. Star CCM+ CFD solver and a wind tunnel with a five hole probe located at University of Limerick were used. The study is an extension of Dr. O'Regan and Dr. Griffin research, O'Regan et al. (2014). Good results in the mean characteristics were achieved only by LES simulation. RANS simulation predicted faster dissipation of a tip vortex and didn't capture a jet-like axial velocity in a vortex core position. High differences in the turbulent characteristics were observed for various turbulent models.*

Keywords: Wing tip vortex, RANS, LES, wind tunnel tests, streamlines turbulence intensity.

1. Introduction, physical description of a wing-tip vortex and literature review

A correct model of downstream tip vortex flow is important for modelling interaction of tip vortex with other object. The origin of the vortex is caused by a pressure difference between upper and down side of a wing. The pressure difference leads to a development of a crossflow velocity. Secondary effect is a development of an axial velocity. The vortex can be divided into three sub-regions, analogous to a turbulent boundary layer over solid walls fig. 1, Zheng & Ramaprian (1993). Region I is viscous core region, region II semi-logarithmic law region and region III defect law region.

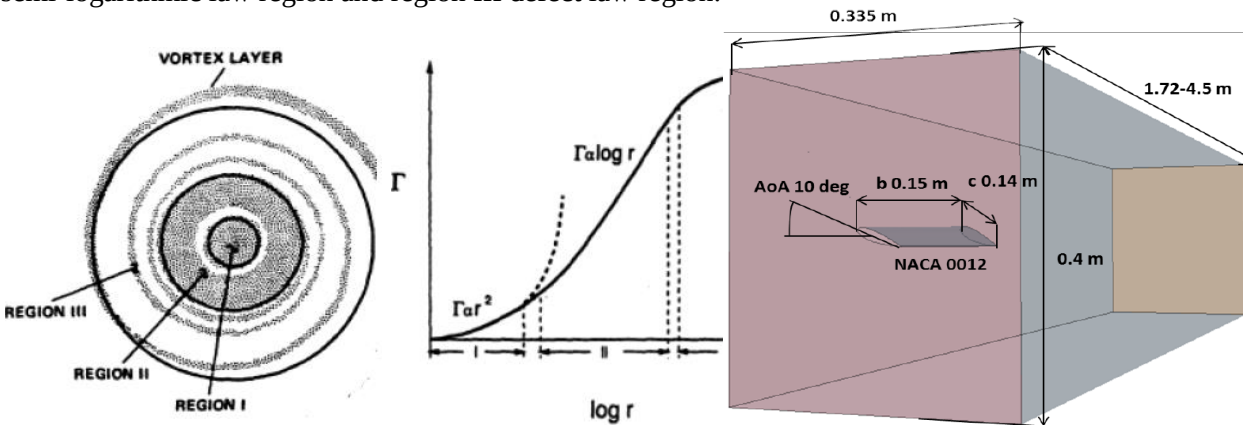

Fig. 1: Left and middle: The structure of the fully developed turbulent vortex Zheng & Ramaprian (1993), Right: Geometry of the wind tunnel and the wing

Results of comprehensive measurements and detail description of physical structure can be found in Chow et al. (1997) and Zheng & Ramaprian (1993). Experimental work was also done in Giuni, & Green (2013) and O'Regan et al. (2014). The tab. 1 shows the survey of performed CFD simulations. While some

[*] Ing. Jiří Matějů.: Institute of Aerospace Engineering, Brno University of Technology, Technická 2896/2; 616 69, Brno; CZ, mateju@lu.fme.vutbr.cz

[**] Dr. Phillip Griffin.: Department of Mechanical, Aeronautical and Biomedical Engineering, University of Limerick; National Technological Park, Limerick, IE, Philip.Griffin@ul.ie

[***] B. E. Jeremiah O'Brien.: Department of Mechanical, Aeronautical and Biomedical Engineering, University of Limerick; National Technological Park, Limerick, IE, Jerry.OBrien@ul.ie

[****] Ing. Pavel Zikmund, Ph.D.: Institute of Aerospace Engineering, Brno University of Technology, Technická 2896/2; 616 69, Brno; CZ, zikmund@lfme.vutbr.cz

of RANS based models were able to capture mean characteristics, high turbulent structure of the tip vortex is possible to capture only by DES, LES or DNS models as can be found in the literature.

Tab. 1: CFD simulations of wing tip vortex. M - mean, T - turbulent characteristics

CFD Method	***Examined***	***Resource***
RANS-SA, SADM, SARC	*M*	*Nash'at et al. (2013)*
LES/ILES, RANS/URANS	*M, T*	*Jiang et al. (2007)*
RST and LES with VC	*M, T*	*O'Regan et al. (2014)*
RANS-SA, DDES	*M*	*Liang & Xue (2014)*
RANS linear EVM, nonlinear EVM, RST-TCL	*M, T*	*Craft et al. (2006)*
RANS - $k-\omega$, DRSM, Hybrid RANS-LES	*M, T*	*Kolomenskiy et al. (2014)*

2. Description of physical conditions, numerical simulations and experiments

International standard atmosphere conditions at 0 m ISA were used. Inlet velocity of $34\ \mathrm{m \cdot s^{-1}}$ was chosen as used at O'Regan et al. (2014) work. Free stream turbulent intensity of 0.5 % was measured in the wind tunnel. The geometry is described in the fig. 1 right. A coordinate system orientation is depicted in the fig. 2 left.

Four different meshes were used for a sensitivity study (tab. 2). Surface mesh was modified by Remesher and Wrapper and refined on the wing edges. A volume mesh was generated by Polyhedral mesher and Optimizer.

Tab. 2: Mesh description (TS – target size, PL – number of prism layers)

Mesh	***Coarser***	***Average***	***Finer***	***Very Fine***
$No.of\ elements$	$2.86 \cdot 10^6$	$4{,}8 \cdot 10^6$	$7 \cdot 10^6$	$10 \cdot 10^6$
$Volumetric\ Control\ TS\ (mm)$	2.8	2.1	1.82	1.68
$TS\ (tunnel/wing)(mm)$	35/1.4	14/2.8	11/1.82	17/1.4
$PL\ (tunnel/wing)$	5/10	0/0	0/4	5/10

Three different CFD turbulent models were tested in Star CCM+ software CD-Adapco (2014); $ANS\ SST\ k-\omega$, $uRANS-RST$ with $0.001\ s$ time step and LES with $10^{-4}\ s$ time step. All the models were used with Vorticity Confinement, All Y+ treatment, constant density gas fluid, segregated flow model and implicit solver.

An open wind tunnel with a closed test section 1 x 0.335 x 0.4 m was used for measurements. Mean characteristics were measured by a five hole probe. Each position was measured for 10 s with a frequency of 1000 Hz on coarse grid (80x80 mm, step 6 mm) and fine grid (40x40 mm, step 2 mm) (fig. 2, middle).

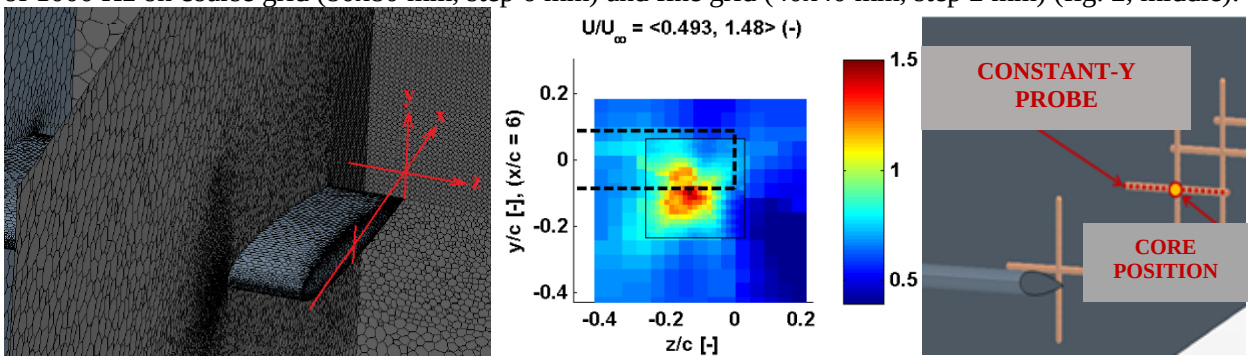

Fig. 2: Left: mesh and coordinate system, Middle: Coarseness of measurement (Normalized axial velocity), Right: Constant y probe position

3. Results

Mean velocity characteristics are evaluated at constant y probe placed at the core position (fig. 2 right). The position of the core is well captured by the all tested models. The fig. 3 left shows a V-component of the normalized velocity at the constant y probe for different turbulent models. The value of the peak V-velocity at the border of the vortex, determined from LES simulation, corresponds to measurements as well as the

velocity gradient in the core. RANS based methods predict more than twice lower peak value. The V-velocity decreases faster outside of the core (in defect law region) in comparison to measurement. The fig. 3 right shows deformation of the vortex core, which is caused probably by wall interference. CFD simulations did not capture the core deformation. Reason can be coarse mesh between volumetric control and the tunnel walls.

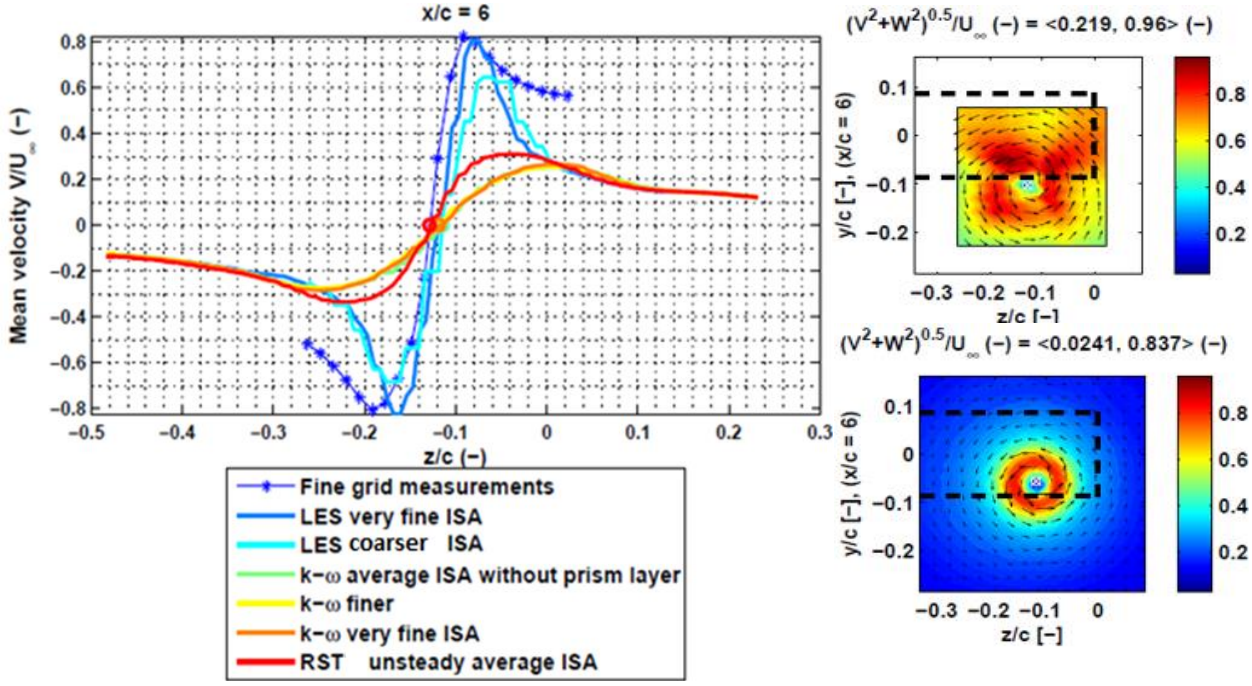

Fig. 3: Left: Different turbulent models and measurement comparison on a V-velocity. Right up: The measured mean crossflow velocity, Right down: LES simulation of the mean crossflow velocity.

The sensitivity study of a normalized mean axial velocity in different models of turbulence and comparison to the measurement can be seen in the fig. 4 left. A Jet-like axial velocity up to 1.5 U_∞ in the core is evident in the measurement. RANS based models do not capture it. The Jet-like velocity is evident also in LES, but not as high as in the measurement. CFD simulation didn't capture a gradient of the axial velocity in a defect law region outside the vortex core. Fig. 4 (right up) shows measured axial velocity, fig. 4 (right down) shows LES axial velocity. LES simulation has potential to capture the jet-like axial velocity profile. Using finer mesh and longer physical time than three seconds could improve the results.

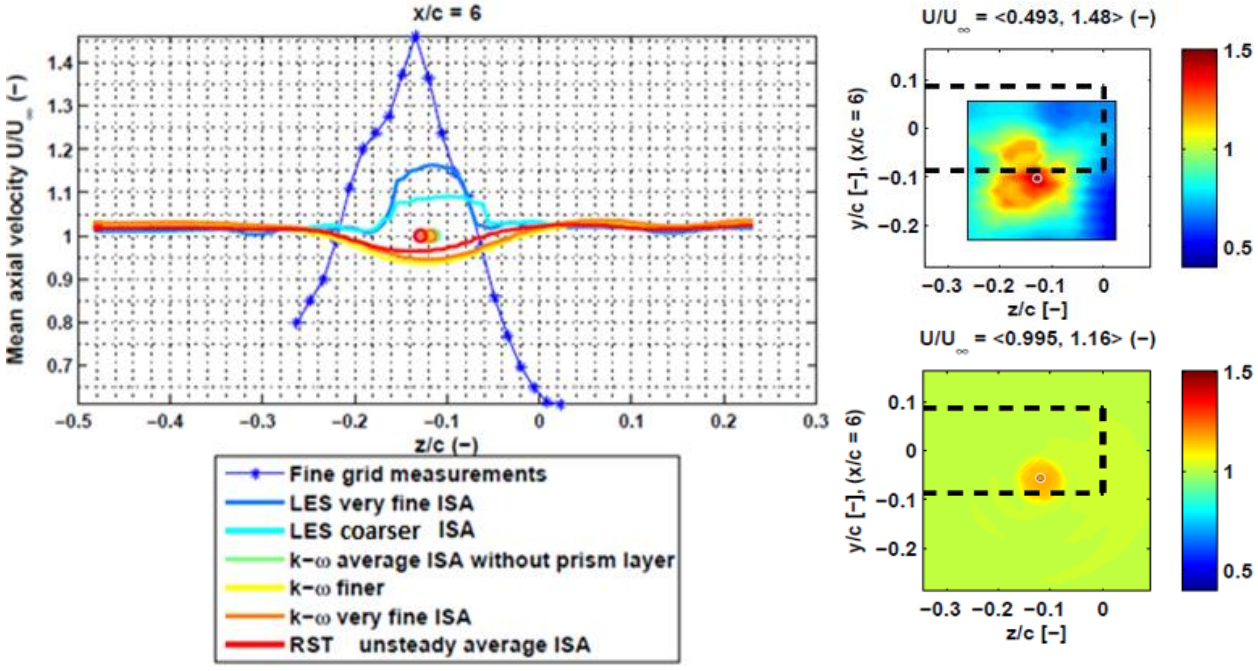

Fig. 4: Left: Different turbulent models and measurement comparison on a mean axial velocity. Right up: The measured mean axial velocity, Right down: LES simulation of the mean axial velocity.

The fig. 5 shows high difference in a turbulent intensity in the core position for different turbulent models. While LES simulation predicts the highest turbulent intensity in the core, $k-\omega$ predicts the highest intensity on a border of the core. Opposite effect (relaminarization) is observed in the core position for uRANS-RST model.

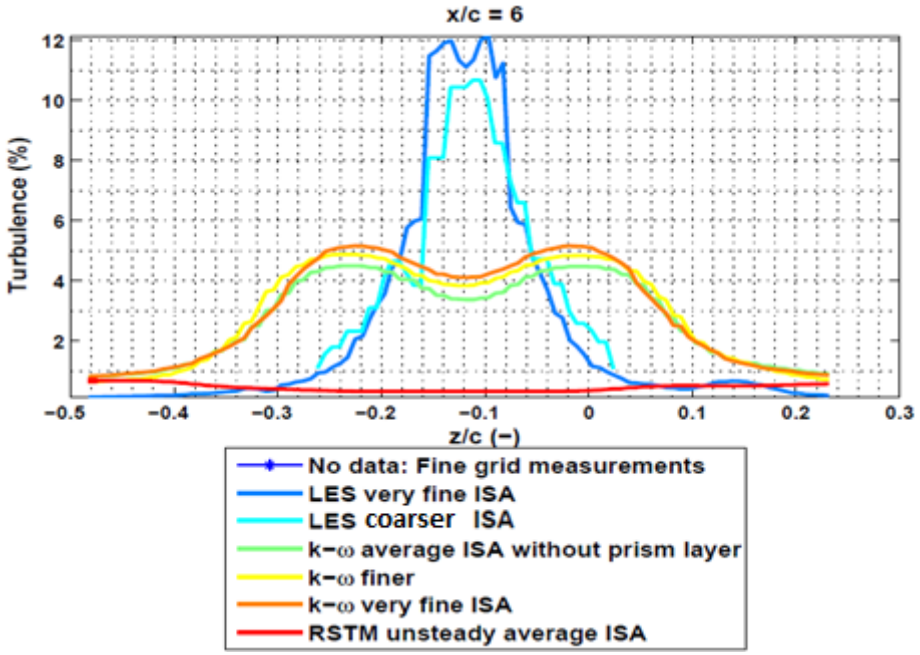

Fig. 5: Different turbulent models results

A streamline development of turbulence intensity for LES simulation (very fine mesh) can be seen in the fig. 6. The red and blue streamlines, which are not in a close contact with the wing have small increase of the turbulent intensity. Highest increase of the turbulent intensity is predicted on the green and yellow streamlines close to a wing tip edges.

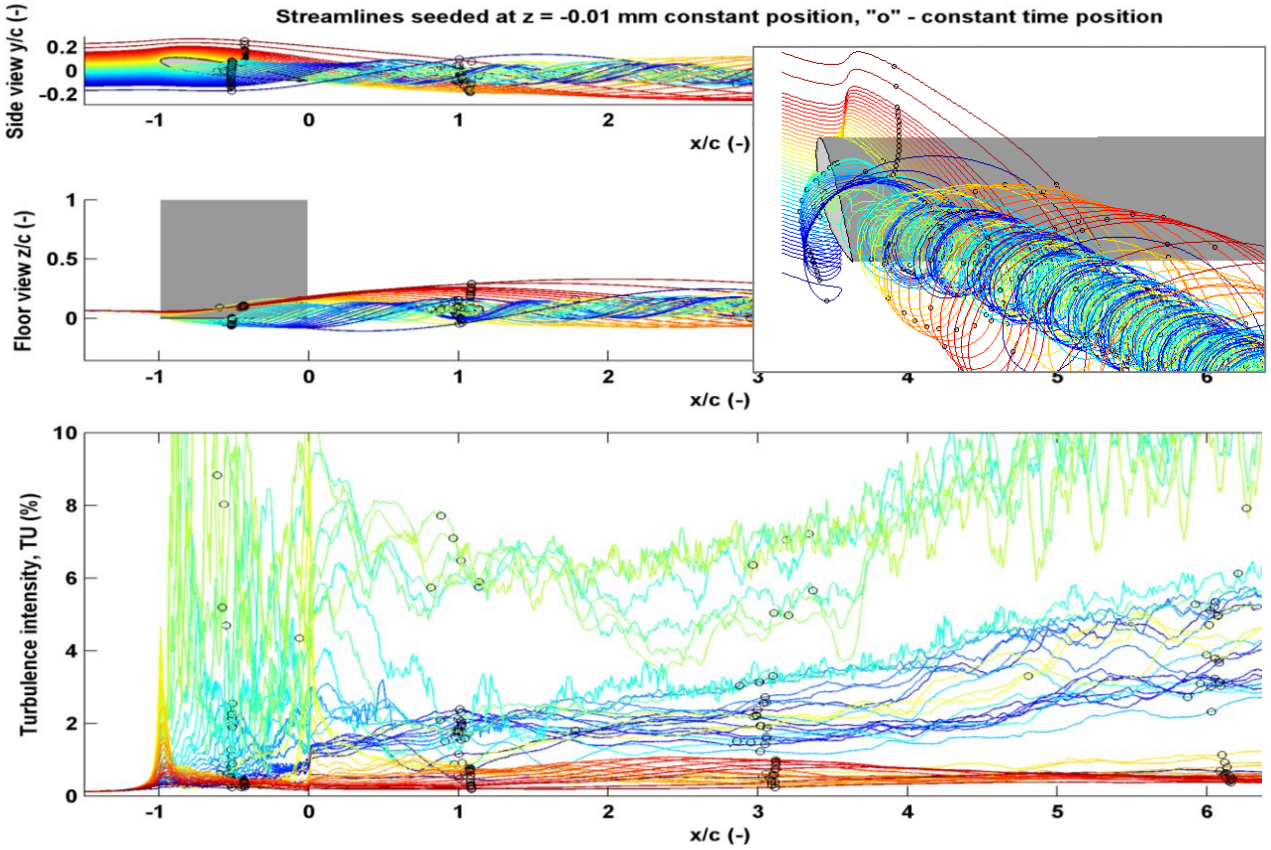

Fig. 6: A turbulent intensity streamlines evolution at $z_{konst} = -0.01m$ coordinate for LES very fine.

4. Conclusion

The study shows different results of the mean characteristics obtained by using different methods. Reasonably good results of the mean characteristics were achieved by LES simulation, although the gradient of crossflow velocity with a core distance outside of the core boundary was much steeper and axial velocity didn't reach the measured peak axial velocity. RANS $k-\omega$ and RST models predicted a lower peak crossflow velocity and did not capture a jet-like axial velocity. Any CFD method didn't capture the core deformation. It can be caused by too coarse mesh between the tunnel walls and volumetric control. The core location was in the same position for the all methods and measurement.

Turbulent intensity in the core depends significantly on various turbulent models. While RST predicted relaminarization, LES and $k-\omega$ predicted increase of the turbulent intensity in the core and with downstream position. High increase of the turbulence intensity is observed only for the streamlines, which are in a close contact to the wing tip edges.

Turbulent intensity is necessary to validate by experiments in future work. Tip edge sharpness influence on turbulence intensity can be studied and mesh density is necessary to increase for LES simulation. Turbulence frequency analysis should be evaluated.

5. Acknowledgement

This study was performed with using of experimental and computer facilities at the University of Limerick.

References

CD-Adapco (2014) User Guide Star-CCM+ Version 9.02.

Chow, J., Zilliac, G. & Bradshaw, P. (1997) Turbulence Measurements in the Near Field of a Wingtip Vortex, NASA Technical Memorandum 110418.

Craft, T. J., Gerasimov A. V., Launder, B. E. & Robinson C. M. E. (2006), A computational study of the near-field generation and decay of wingtip vortices, International Journal of Heat and Fluid Flow, 27, 4, 684-695.

Giuni, M. & Green, R. B. (2013) Vortex formation on squared and rounded tip, Aerospace Science and Technology, 29, 1, 191-199.

Jiang, L., Cai, J. & Liu, C. (2007) Large-eddy simulation of wing tip vortex in the near field, Tech. rep., University of Texas.

Kolomenskiy, D., Paoli, R. & Boussuge, J. F. (2014) Hybrid RANS-LES simulation of wingtip vortex dynamics, 4th Joint US-European Fluids Engineering Division Summer Meeting and 12th International Conference on Nanochannels, Microchannels, and Minichannels, Chicago, Illinois, USA, ASME, 11.

Liang, Z. C. & Xue, L. P. (2014) Detached-eddy simulation of wing-tip vortex in the near field of NACA 0015 airfoil, Journal of Hydrodynamics, Ser. B, 26, 2, 199-206.

Nash'at, N. A. Proctor, F. H. & Perry, R. B. (2013) Numerical Simulation of the Aircraft Wake Vortex Flowfield, 5th AIAA Atmospheric and Space Environments Conference, American Institute of Aeronautics and Astronautics.

O'Regan, M. S., Griffin, P. C. & Young, T. M. (2014) Numerical and experimental investigation of the mean and turbulent characteristics of a wing-tip vortex in the near field, Proceedings of the Institution of Mechanical Engineers Part G: Journal of Aerospace Engineering, 228, 13, 2516-2529.

O'Regan, M. S., Griffin, P. C. & T. M. Young. (2014): A Vorticity Confinement Model Applied to URANS and LES Simulations of a Wing-tip vortex in the Near-field, unpublished.

Zheng, Y. & Ramaprian, B. R. (1993) An Experimental Study of Wing Tip Vortex in the Near Wake of Rectangular Wing.

Abbreviations

LES, ILES	Large Eddy Simulation, Implicit LES	$k-\omega$	$k-\omega$ turbulent model
DES, DDES	Dettached Eddy simulation, Delayed DES	SST	Menter's Shear Stress Transport
DNS	Direct numerical simulation	RST	Reynolds stress transport model
ISA	International standard atmosphere	SGS	Subgrid-scale model
uRANS	unsteady RANS	WALE	Wall-Adapting-Local-Eddy-Viscosity
SA	Spallart - Allmaras	$\overline{v_i}$	velocity vector
SADM	SA with Dacles-Mariani correction	Re	Reynolds number
SARC	SA with Splart-Shur correction	AoA	Angle of Attack
VC	Vorticity confinement or Volumetric control	Tu	Turbulence intesity
EVM	Eddy-viscosity model	U_∞	Free-stream velocity
TCL	two-component limit	$\Delta\bar{l}_i$	*s*egment length along the square path surrounding the vortex

Nomenclature

Description	**Symbol / Equation**	**Normalization**
Mean stream-wise (axial) velocity	U	$/U_\infty$
Mean cross-flow velocity	$\sqrt{V^2+W^2},$	$/U_\infty$
Velocity magnitude	$\sqrt{U^2+V^2+W^2}$	$/U_\infty$
Vortex core radius	r_c	$/c$
Trajectory of the vortex core	x_c, y_c, z_c	$/c$
Jet/wake-like axial velocity	$-$	$-$
Vortex circulation (strength)	$\Gamma=\sum_i \overline{v_i}\Delta\bar{l}_i$	$/(U_\infty \cdot c)$
Stream-wise vorticity	$\omega_x = \partial W/\partial y - \partial V/\partial z$	$\cdot\, c/U_\infty$
RMS Reynolds stress component velocity	$\overline{u'^2}, \overline{v'^2}, \overline{w'^2}$ $\overline{u'v'}, \overline{u'w'}, \overline{v'w'}$	$/U_\infty^2$
Velocity gradients of U, V, W with x, y, z	$\partial U_i/\partial x_i$	
Velocity gradient with core distance	$\partial(V_t/R)/\partial R$	
Temperature	T	
Kinetic energy per unit mass	$k=\frac{1}{2}\cdot(\overline{u'^2}+\overline{v'^2}+\overline{w'^2})$	$Tu=\frac{\sqrt{\frac{2}{3}\cdot k}}{U_\infty}$
Total pressure	P_t	$(P_t-P_\infty)/\frac{1}{2}\rho U_\infty^2$
Pressure gradient with x, y, z	$\partial P/\partial x_i$	
Static pressure	P_s	$(P_s-P_\infty)/\frac{1}{2}\rho U_\infty^2$
Time	t	$/(U_\infty \cdot c)$

Radial and tangential components of velocities with respect to the core positions are more suitable for some problems:

$$y = r\cdot\cos(\Theta), \quad V = V_r\cdot\cos(\Theta) - V_\mathrm{t}\cdot\sin(\Theta) \tag{1}$$

$$z = r\cdot\sin(\Theta), \quad W = V_r\cdot\sin(\Theta) + V_t\cdot\cos(\Theta) \tag{2}$$

A core radius r_c of a wing tip vortex is a distance between the minimum and maximum cross-flow velocity in a vortex centre.